SURGERY FOR CONGENITAL HEART DISEASE

USE OF COMPUTATIONAL FLUID DYNAMICS IN THE DESIGN OF SURGICAL PROCEDURES: APPLICATION TO THE STUDY OF COMPETITIVE FLOWS IN CAVOPULMONARY CONNECTIONS

M. R. de Leval, MD, FRCS[a]
G. Dubini, PhD[c§]
F. Migliavacca[c§]
H. Jalali, MD[a§]
G. Camporini[a§]
A. Redington[b§]
R. Pietrabissa, PhD[c§]

Computational fluid dynamic methods based on a finite-element technique were applied to the study of (1) competition of flows in the inferior and superior venae cavae in total cavopulmonary connection, and (2) competition between flow in the superior vena cava and forward flow from a stenosed pulmonary artery in bidirectional cavopulmonary anastomosis. Models corresponding to various degrees of offsetting and shape of the inferior vena caval anastomosis were simulated to evaluate energy dissipation and flow distribution between the two lungs. A minimal energy loss with optimal flow distribution between the two lungs was obtained by enlarging the inferior vena caval anastomosis toward the right pulmonary artery. This modified technique of total cavopulmonary connection is described. A computational model of the operation was developed in an attempt to understand the mechanisms of postoperative failure. In tight pulmonary artery stenosis (75%), the pulsatile forward flow is primarily directed to the left pulmonary artery, with little influence on superior vena caval pressure and the right pulmonary artery. Pulsatile forward flows corresponding to 15%, 30%, 45%, and 60% of the systemic artery output increased the mean pulmonary artery and superior vena caval pressures by 1, 1.7, 2.4, and 3.6 mm Hg, respectively. Although the modeling studies were not able to determine the cause of postoperative failure, they emphasize the impact of local geometry on flow dynamics. More simulations are required for further investigation of the problem. (J THORAC CARDIOVASC SURG 1996;111:502-13)

Complex flow problems in fields as varied as meteorologic calculation, geophysical fluid dynamics, astrophysical fluid dynamics, flow machinery, and design of aircraft, ships, and automobiles are now studied with numeric methods by means of digital computers. One of the most commonly used methods in computational fluid dynamics (CFD) is the finite-element method (FEM). FEM modeling techniques have been applied to biomedical problems for a number of years. We postulate that CFD technology could usefully be applied to the design and refinement of a number of surgical procedures aimed at mending cardiovascular anomalies.

We tested this hypothesis in two specific clinical situations. (1) One area studied was the flow competition between the superior vena cava (SVC) and inferior vena cava (IVC) in total cavopulmonary connection (TCPC). This is in line with the in vitro modeling and open-channel visualization studies that had led us to recommend the TCPC.[1] (2) The other area studied was flow competition between the SVC flow from a bidirectional cavopulmonary anastomosis (BCPA) and an additional source of

From the Great Ormond Street Hospital for Children, NHS Trust,[a] London, and the Royal Brompton National Heart and Lung Institute,[b] and the Dipartimento di Bioingegneria, Politecnico di Milano,[c] Milan, Italy.

Supported by grant No. PG/92141 from the British Heart Foundation.

Read at the Seventy-Fifth Annual Meeting of The American Association for Thoracic Surgery, Boston, Mass., April 23-26, 1995.

Address for reprints: M. R. de Leval, MD, FRCS, Cardiothoracic Unit, Great Ormond Street Hospital for Children, London WC1N 3JH, United Kingdom.

[§]By invitation.

0022-5223/96 $5.00 + 0 **12/6/69256**

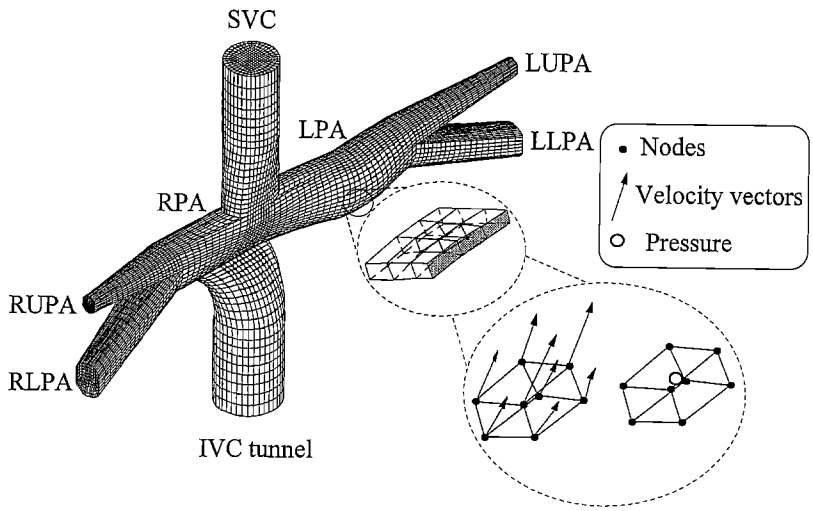

Fig. 1. Diagram of a FEM mesh of the TCPC model. The insets show the finite elements with low presentation of an eight-node (three-dimensional) isoparametric brick element with locations for velocity vectors and for pressure calculation in another element. *LUPA,* Left upper pulmonary artery; *LLPA,* left lower pulmonary artery; *RUPA,* right upper pulmonary artery; *RLPA,* right lower pulmonary artery.

pulmonary blood flow (ABF). Clinical recommendations based on the flow simulation studies were made and the preliminary results are reported here. Potential applications of CFD technology to cardiovascular sciences are discussed.

CFD modeling

Governing equations for flows of practical interest are usually so complicated that an analytic solution is unavailable, and it is therefore necessary to seek a computational solution. The mathematic equations (the unsteady Navier-Stokes equations) are replaced by algebraic equations so that a computer can be used to obtain the solution. The process of converting the continuous model into a discrete model of algebraic equations is called *discretization.* All methods of discretization involve an approximation that approaches the true continuum solution as the number of discrete variables increases. The FEM is a method of discretization where the flow domain is divided into a number of simply shaped regions called *finite elements.* Within each element, a certain number of points or nodes are defined where the numeric value of the unknown functions, and eventually their derivatives, will have to be determined (Fig. 1). The space discretization consists in setting up a mesh or a grid in which the continuum of space is replaced by a finite number of elements.

Flow competition in the TCPC

Clinical problem. In basic flow dynamic terms, a TCPC represents two T-junctions with flow velocities in opposite directions from SVC and IVC into the pulmonary arteries. Those abrupt changes in geometry and velocity inevitably generate energy losses. Furthermore, postoperative cineangiograms demonstrate that the SVC flow, which carries approximately one third of the systemic venous return, goes preferentially to the bigger right lung, whereas the IVC flow, which carries approximately two thirds of the systemic venous return, goes mainly to the smaller left lung. This study was aimed toward improving the design of the operation to reduce energy loss and optimize flow distribution between the two lungs.

CFD studies. Anatomic and hemodynamic variables necessary to construct and validate the three-dimensional models of the investigated domains were obtained from angiocardiograms and cardiac catheterization data. The developed three-dimensional geometric models for TCPC and BCPA simulations are fully parametric; that is, all their dimensions are mathematically related to a basic set of about 30 measurements estimated from the angiocardiograms and corrected on the basis of the magnification factor (computed as the ratio between the measured catheter diameter on the angiocardiographic frames and its actual diameter). Anteroposterior and lateral views were used to obtain the measurements and to build the three-dimensional geometries of the reference models. A commercial CFD code (FIDAP; Fluid Dynamics International, Evanston, Ill.) was used to compute the fluid dynamic variables (pressure and velocity components). This code combines the FEM and the Galerkin method of weighted residuals to solve the full Navier-Stokes equations. The geometric models were fully parametric. The FEM mesh was made of three-dimensional brick elements containing eight nodes; quadrilateral two-dimensional elements with four nodes were used at the inlet and outlet sections and along the walls. The number of nodes for each model ranged from 15,000 to 33,000. In addition to the three-dimensional computational model, a lumped parameter model of the afterload, representing the two lungs and the left atrium, was developed. A pulmonary

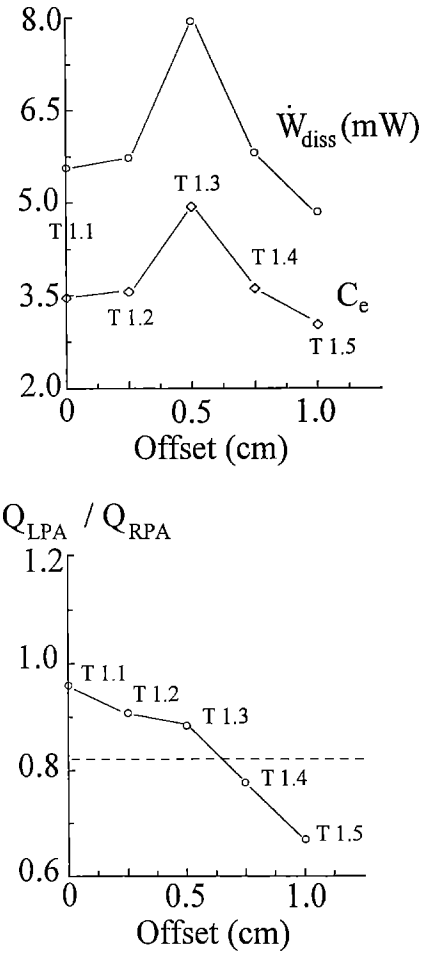

Fig. 2. *Upper panel* shows $\dot{W}_{diss}$ and C_e as functions of the offset of the caval anastomosis in the first series of TCPC simulations. Flow distribution between the two lungs is represented in the *lower panel.* Width of both caval anastomoses is kept constant at 1.5 cm. The *dashed line* represents the ratio corresponding to the assumed normal flow rates through both lungs (45% to the left and 55% to the right).

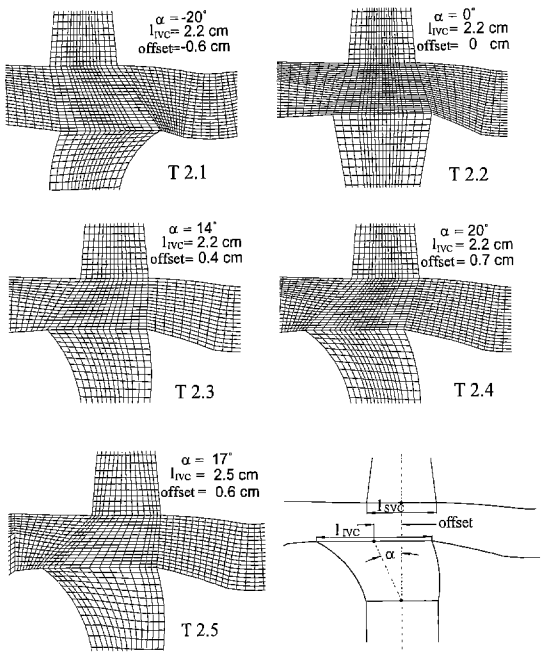

Fig. 3. Details of the mesh of the TCPC models in which the IVC anastomosis is enlarged with a range of offsets (second series). Width of the SVC anastomosis is kept constant at 1.5 cm; width of the IVC anastomosis (l_{IVC}) is 2.2 cm except in model T2.5, where it is 2.5 cm.

arteriolar resistance of 1.62 Wood units (millimeters of mercury per liter per minute) and a left atrial pressure of 4 mm Hg were selected for the simulations reported on here. A FORTRAN program was written to obtain the parametric construction and the mesh of the three-dimensional simulations and to connect the two computational models, with the calculated afterload used as the boundary conditions for the three-dimensional model. The computations were done on an IBM RISC-6000 Model 340 workstation (International Business Machines Corp., Armonk, N.Y.) with 32 Mb RAM. Detailed descriptions of the methods and their limitations have been previously reported[2, 3] and are summarized in Appendixes 1 and 2.

The grid of the TCPC model is represented in Fig. 1. Flow distributions between the left and the right lung were qualitatively studied with particle path plots and calculated from velocity vector plots. In a particle path plot, a massless particle is introduced at some point in the flow domain and the path of motion of the particle is tracked on the basis of the computed flow field. Two energetic indexes were calculated[4]: the hydraulic dissipated power, $\dot{W}_{diss}$, which is the difference between the total energy at the inlet and at the outlet of the domain, and the total energy-loss coefficient, C_e, which is the ratio between the hydraulic dissipated power and the inlet kinetic energy (Appendix 2). Two sets of simulations were carried out. In the first series, an IVC anastomosis with the same diameter as the SVC anastomosis was displaced alongside the pulmonary artery while the position of the SVC anastomosis was kept constant. Results are reported as functions of the offset, which represents the distance between the centers of the two caval anastomoses measured toward the right pulmonary artery axis. The offset is negative if the center of the anastomosis of the IVC is displaced toward the reader's right side. The best flow distribution between the right and the left lung, considered to be 55% to the right lung and 45% to the left, was obtained for an offset of the IVC anastomosis of 0.5 to 0.7 cm toward the right pulmonary artery. Unfortunately, this corresponds to the maximum energy dissipation (Fig. 2). In an attempt to improve the balance between flow distribution and energy dissipation, the IVC anastomosis was enlarged and moved alongside the pulmonary artery (Fig. 3). The results of those simulations are summarized in Table I. A minimal loss of energy was obtained by angling the IVC anastomosis toward the right pulmonary artery (model T2.5, α =

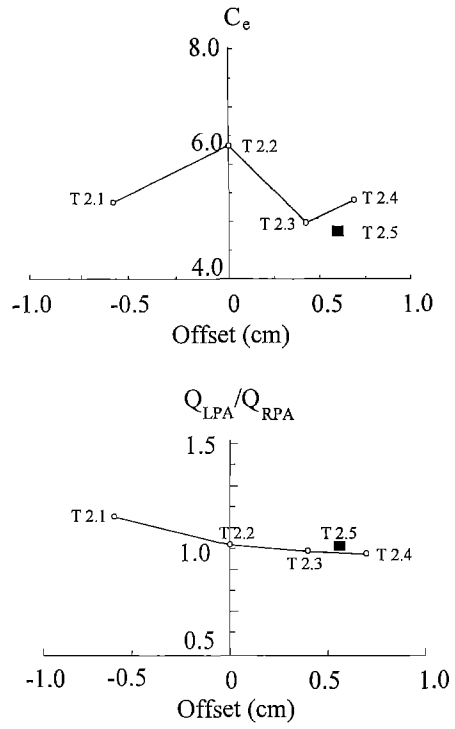

Fig. 4. C_e and flow distribution as a function of the offset and of the enlargement of the IVC anastomosis in the second series of TCPC simulations. *Open circles* refer to the models with IVC anastomoses of 2.2 cm; the *solid rectangles* refer to the model with IVC anastomosis of 2.5 cm.

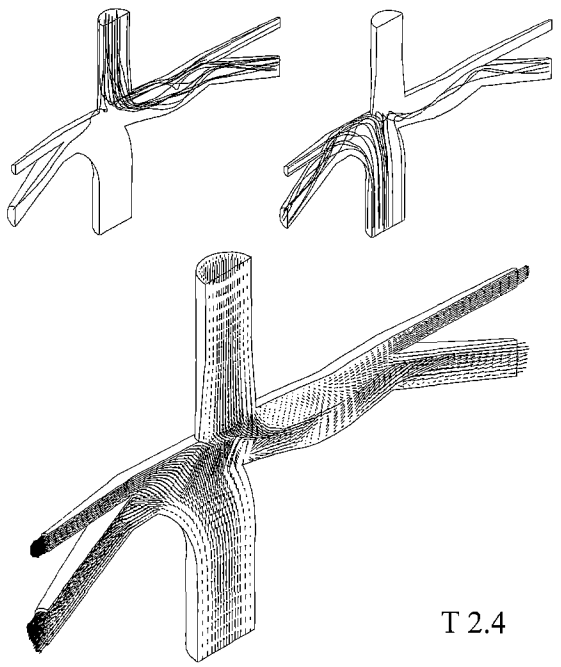

Fig. 5. Particle path plots and velocity vector map for the TCPC model with enlargement of the IVC anastomosis toward the right pulmonary artery (IVC anastomosis width of 2.2 cm and offset of 0.7 cm).

Table I. *Results of the second series of TCPC simulations*

	Offset (cm)	l_{IVC} *(cm)*	α *(degrees)*	Q_{LPA} *(L/min)*	Q_{RPA} *(L/min)*	Q_{LPA}/Q_{RPA}	P_{SVC} *(mm Hg)*	P_{IVC} *(mm Hg)*	P_{LPA} *(mm Hg)*	P_{RPA} *(mm Hg)*	C_e	$\dot{W}_{diss}/\dot{W}_{in}$ *(%)*
Model T 2.1	−0.6	2.2	−20	1.59	1.38	1.15	8.7	8.3	6.5	6.9	5.4	15.2
Model T 2.2	0.0	2.2	0	1.49	1.48	1.00	8.9	8.7	6.8	6.8	6.3	17.3
Model T 2.3	0.4	2.2	14	1.48	1.49	0.99	8.6	8.4	6.8	6.8	5.0	14.1
Model T 2.4	0.7	2.2	20	1.47	1.50	0.98	8.8	8.5	6.8	6.8	5.3	14.8
Model T 2.5	0.6	2.5	17	1.49	1.48	1.00	8.7	8.4	6.8	6.8	4.9	13.9

l_{IVC}, Width of the IVC anastomosis. Other abbreviations as given in the appendixes.

17 degrees, width of IVC anastomosis 2.5 cm), and this corresponds to a flow ratio between the right and the left lung of just above 1 (Fig. 4). The particle path and the vector velocity plots (Fig. 5) showed that the SVC drains preferentially to the left lung whereas the IVC drains preferentially to the right lung, the opposite of the pattern usually observed angiocardiographically after the classical Fontan or TCPC operation. In terms of fluid dynamics, the enlargement of the IVC anastomosis acts as a diffuser or recuperator, which is a device used in hydraulic plants to reduce dissipation of kinetic energy at abrupt changes of cross-section. There is an optimum range of angles for which the decrease of head loss is maximal (α = 14 to 17 degrees, models T2.3 and T2.5).

Clinical inferences. As a result of these modeling studies, we have altered the surgical technique of the TCPC. The IVC anastomosis is now enlarged toward the right pulmonary artery. If the pulmonary arteries are large, the main pulmonary artery may simply be ligated and the pulmonary incision made on the inferior aspect of the right pulmonary artery. More often, we transect the main pulmonary artery and fully mobilize both branches to the pulmonary hilus, with division of the ligamentum arteriosum to bring the distal end of the transected pulmonary artery toward the SVC. The distal opening of the main pulmonary artery is then extended toward the inferior aspect of the right pulmo-

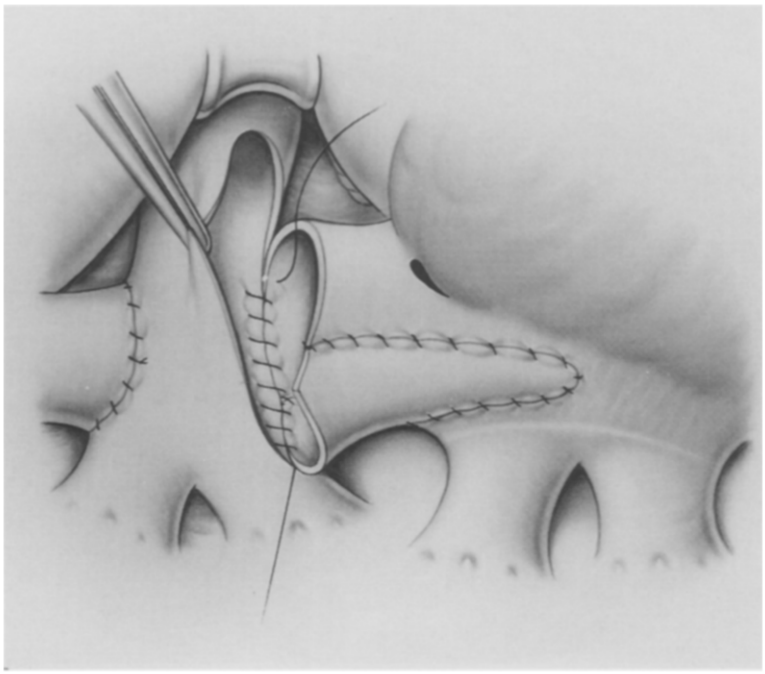

Fig. 6. Illustration of the surgical technique of patch enlargement of the IVC anastomosis with a lateral polytetrafluoroethylene patch.

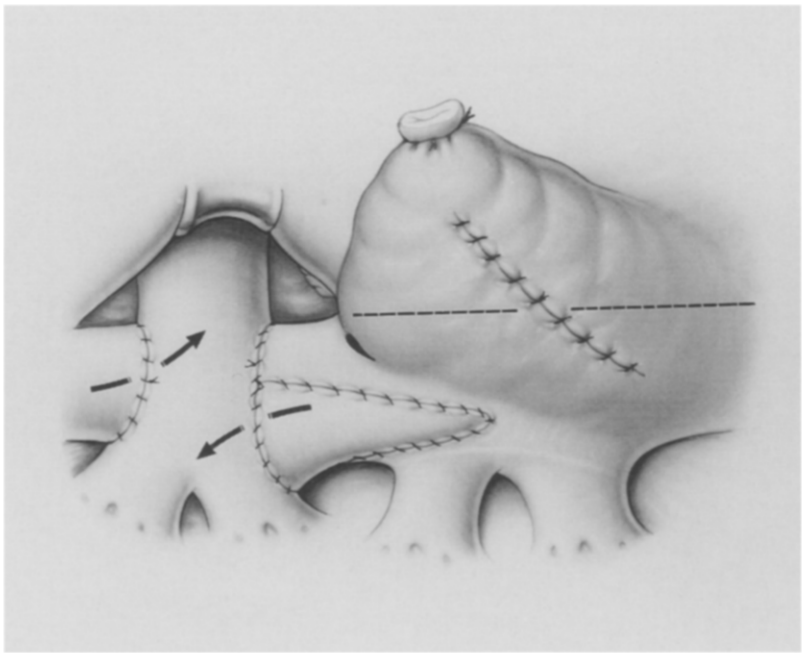

Fig. 7. Modified TCPC completed.

nary artery. A longitudinal incision is made on the lateral aspect of the transected end of the SVC into the sinus venarum. The incision is carried down between the sulcus terminalis and the Waterston groove a distance of 1.5 to 2.00 cm. A triangular patch of polytetrafluoroethylene vascular graft trimmed from a 6 to 8 mm conduit is sewn into the incision. The patch extends beyond the level of the transection of the SVC

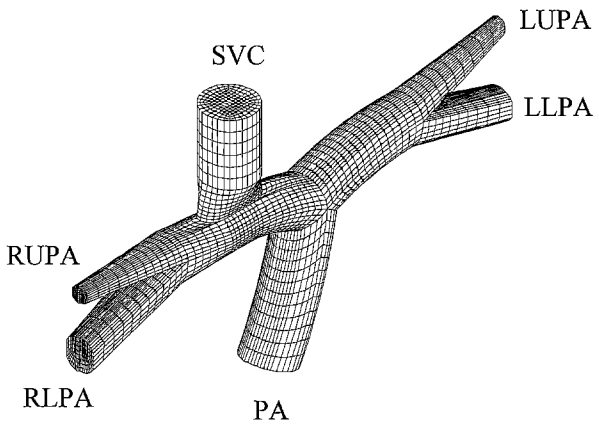

Fig. 8. Grid of BCPA with forward flow from the native pulmonary artery.

to widen the section area of the anastomosis and to angle it to the right pulmonary artery. The anastomosis between the SVC and the pulmonary artery is then constructed (Figs. 6 and 7). The cavoatrial incision is situated behind and well away from the sinus node; there is, however, a potential risk of damaging the sinus node's blood supply if the sinus node artery passes behind the origin of the SVC before reaching the sinus node. To date, the incidence of temporary supraventricular arrhythmias has not been different from that seen after the "classic" TCPC. One patient with a complex atrioventricular discordance, however, had persistent episodes of junctional rhythm, for which a pacemaker was inserted. Whether this is related to a vascular injury to the sinus node artery has not been determined. Meanwhile, it may be advisable not to make a lateral incision when the sinus node artery is seen to have a posterior pathway.

Flow competition in the BCPA

The clinical problem. The BCPA is used as a staged procedure or a definitive palliation in the treatment of hearts with a single ventricular chamber. An ABF arising from either the native pulmonary outflow tract or from a systemic–pulmonary artery shunt is often maintained to provide a better (higher oxygen saturation) and longer palliation. Setting aside concerns about volume load on the ventricular chamber, the preoperative clinical problem is often to know what magnitude of ABF is acceptable while constructing a BCPA. In fluid dynamic terms, the operation creates a competition in the pulmonary arteries between the continuous flow from the SVC and the pulsatile flow from the ABF. CFD was applied to analyze the flow dynamic effects of such a competition and to see whether they correlated with the postoperative morbidity associated with the surgical procedure.

CFD studies. The same computational approach used to study flow competition in the TCPC was used in the study of flow competition in the BCPA. The grid of a BCPA model with forward flow from the main pulmonary artery is represented in Fig. 8. The geometry of the flow

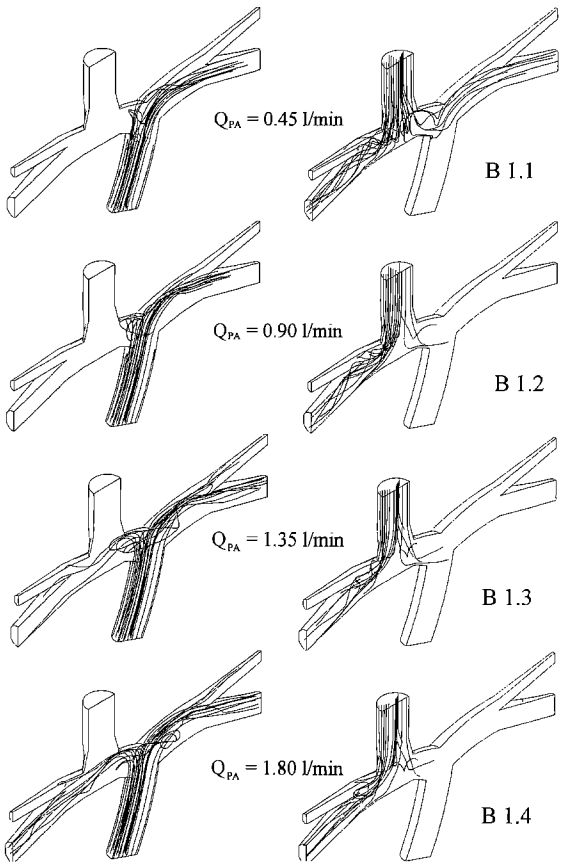

Fig. 9. Particle path plots with injection of the tracer from pulmonary artery *(left)* and SVC *(right)* in the BCPA and ABF models (without pulmonary stenosis).

domain was obtained from angiocardiograms of hearts with ventriculoarterial concordance, where the main pulmonary artery is "pointing" toward the left lung. A steady flow was imposed on the SVC with a fully developed parabolic velocity profile, whereas a pulsatile flow was introduced into the native pulmonary artery. Waveforms obtained from multiple-catheterization data of pulmonary stenosis of variable severity were used to simulate forward flow. Two sets of simulations were carried out to differentiate the effects of forward flow and flow configuration on the pulmonary arterial branches and the SVC. The flow from the SVC was kept constant (1 L/min) for all the simulations, and a heart rate of 120 beats/min, with a systolic and diastolic time of equal duration, was selected. In the first set of simulations, forward flows of 0.45, 0.90, 1.35, and 1.80 L/min were tested. Forward flows of 1.0 and 1.8 L/min through discrete valvular and discrete supravalvular (banded pulmonary artery) stenoses of different degrees were tested in the second set of simulations. Particle path plots and velocity vector plots were constructed and used to derive flow dynamics. Without stenosis, increments in forward flows altered the distribution of the caval and the forward flow between the two lungs. There is a preferential distribution of the forward

Table II. *Results of the BCPA simulations without pulmonary stenosis*

	Mean Q_{PA} (L/min)	Constant Q_{SVC} (L/min)	P_{PA} (mm Hg)			P_{SVC} (mm Hg)			Mean Q_{LPA} (%)	Mean Q_{RPA} (%)	Mean Q_{LPA}/Q_{RPA}
			Maximum	Mean	Minimum	Maximum	Mean	Minimum			
Model B 1.1	0.45	1.00	7.3	6.3	5.4	7.8	6.4	6.0	51.9	48.1	1.1
Model B 1.2	0.90	1.00	9.4	7.1	5.6	8.3	7.2	6.4	52.3	47.7	1.1
Model B 1.3	1.35	1.00	11.7	7.8	4.7	10.0	7.8	6.6	52.7	47.3	1.1
Model B 1.4	1.80	1.00	12.9	8.5	4.1	10.8	8.6	6.6	52.5	47.5	1.1

Abbreviations as given in the appendixes.

Table III. *Results of the BCPA simulations with pulmonary stenosis*

	Mean Q_{PA} (L/min)	Constant Q_{SVC} (L/min)	Degree of stenosis (%)	Mean Q_{LPA} (%)	Mean Q_{RPA} (%)	Mean Q_{LPA}/Q_{RPA}
Model B 1.2	0.9	1.0	0	52.3	47.7	1.1
Model B 2.1	0.9	1.0	60	64.9	35.1	1.8
Model B 2.2	0.9	1.0	75	68.4	31.6	2.2
Model B 1.4	1.8	1.0	0	52.5	47.5	1.1
Model B 2.5	1.8	1.0	75	73.7	26.3	2.7

Abbreviations as in the appendixes.

flow to the left lung, and consequently a higher peak velocity in the left pulmonary artery (Fig. 9). The overall flow ratio between the two lungs, however, remains constant at 1.1 (Table II). With discrete valvular stenosis, the proportion of flow going to the left lung increases as the stenosis becomes more severe. With a forward flow of 1.8 L/min and a stenosis of 75%, nearly three quarters of the blood goes to the left lung (Table III). This implies that during systole a greater proportion of the forward flow goes to the left lung and in diastole a greater proportion of the caval flow also goes to the left lung. This preferential flow to the left lung is less marked with supravalvular discrete stenosis. The ABF has only a moderate influence on the mean SVC pressure, which increases from 6.4 to 8.6 mm Hg when the forward flow rises from 0.45 to 1.8 L/min.

Compilation of clinical and CFD data. From January 1988 to December 1994, 107 patients underwent BCPA and ABF. Failures—described as need for reoperation as a result of excessive pulmonary flow (in nine patients), SVC pressure greater than 18 mm Hg (in six patients), pleural effusion lasting more than 1 week (in three patients), or chylothorax (in six patients)—occurred in 24 patients (22.4%). The preoperative and postoperative hemodynamic data of those whose treatment failed and those whose treatment did not fail are displayed in Table IV. There was no statistical difference between the two groups. Within the range of preoperative flows and pressures of patients subjected to BCPA and ABF, it was not possible to predict outcome and complications.

Assuming cardiac output of 3 L/min and SVC flow of 1 L/min, computational modeling studies indicate that an ABF leading to an overall ratio of pulmonary to systemic flow of up to 1 should be well tolerated in terms of pressure increment in the pulmonary artery and the SVC. For a given ABF, the pulmonary flow dynamics are affected by the severity and the position of the stenosis. The actual geometry of the flow domain appears to be of great importance. The angle of the main pulmonary artery and its branches is known to vary greatly from one condition to another. For example, in transposition of the great arteries the main pulmonary artery often points toward the right pulmonary artery. Diffuse pulmonary stenosis may influence pulmonary flow fields differently than discrete stenosis. More simulations are therefore required for a better understanding of the effect of local geometry on flow dynamics. Simulations of extreme stenosis (90%) were attempted but so far remain inconclusive because of the creation of transitional flow between laminar and turbulent flows. Reynolds and Womersley numbers reached were 6726 and 2.5, respectively.[5] Pulmonary vascular resistance is expected to be one of the main determinant factors of postoperative hemodynamics. Pulmonary vascular resistance was not directly measured before operation. A preoperative resistance index (mean pulmonary arterial pressure divided by the ratio of pulmonary to systemic flow) was found to have no correlations with outcomes. This obviously indicates that patients with elevated pulmonary vascular resistance were not subjected to BCPA plus ABF. The reason that some patients have a complicated postoperative course remains unclear and warrants further investigation.

Discussion

The science of fluid dynamics started with Newton. The governing equations for Newtonian fluid dynamics, the unsteady Navier-Stokes equations, were formulated more than 150 years ago. The steady improvement in the speed of computers and their memory size since the 1950s has led to the emergence of CFD as a means of modeling real flows. In the cardiovascular system, the goal of CFD studies is to predict flow, pressure, and velocity

Table IV. *Comparative hemodynamic data of patients who underwent BCPA plus ABF with and without postoperative failure*

	With failure		*Without failure*	
Hemodynamics	*Mean*	*95% CL*	*Mean*	*95% CL*
Preoperative aortic saturation (%)	81	68-94	79	65-93
Postoperative aortic saturation (%)	90	75-99	90	78-100
Preoperative PAP (mm Hg)	14.1	5-22	13.7	5-25
Postoperative PAP/QPQS	0.95	0.2-2.7	1.14	0.3-3.6

CL, Confidence limits; *PAP,* pulmonary arterial pressure; *QPQS,* ratio of pulmonary to systemic flow.

fields as a function of time and position in a realistic model of the domain under investigation. The technology has been applied to the study of the normal cardiovascular system[6, 7] and to the design of prosthetic devices.[8] With few exceptions, such as the simulation of the fluid dynamics of an aorta-coronary bypass,[9] CFD has rarely been applied to the actual design and refinement of interventions on the cardiovascular system.

As far as the methodology is concerned, important assumptions are made to generate appropriate models and to solve the equations that predict flow distribution. We are currently looking at the possibility of directly translating three-dimensional geometries from magnetic resonance imaging to computer-aided design formats transferable to FEM packages. This direct translation would avoid the phase of mesh creating by means of a specially written FORTRAN program.

The clinical implications of the simulation studies of the competitive flow in cavopulmonary anastomoses presented in this article are still preliminary. Flow distribution studies between the two lungs should be validated. This could be assessed by nuclear magnetic resonance velocity mapping by the technique described by Rebergen and associates.[10] In the TCPC, one could conceive ways to obtain an even more favorable flow pattern by placing a second angulation patch on the medial aspect of the SVC–pulmonary artery anastomosis to direct more SVC blood to the left lung. The flow simulation studies are quite convincing in demonstrating that it is not necessary to divide the right pulmonary artery and anastomose the SVC to its proximal end and the IVC to its distal end to obtain a more physiologic distribution of pulmonary blood flows.[11] Such a procedure loses the flexibility of the BCPA cavopulmonary anastomosis, which could become useful if, for example, the pulmonary vascular resistance in one lung were to increase or one of the anastomoses were to become restrictive. In addition the left lung, being deprived of IVC blood, might be at higher risk for development of arteriovenous fistulas (the so-called hepatic factor).

The purpose of this article is not to discuss the pros and cons of ABF in construction of a BCPA. ABF is an optional solution for patients who are likely to become good candidates for a Fontan circulation. It is a more logical solution for those patients who are not optimal candidates or whose anatomy will not be suitable for the Fontan operation. Two recent reports[12, 13] have shown that BCPA with ABF had a higher postoperative morbidity rate than BCPA without ABF. This difference must be related to flow dynamic problems. Although we have been unable to define these problems so far, the modeling studies have shown the important effects of local geometry on flow dynamics and flow distribution between the two lungs, and more simulations are needed to attempt to elucidate the problem. The concept of BCPA with forward flow from the native pulmonary artery has also been applied to a subset of patients with a small right ventricle and intact ventricular septum without pulmonary stenosis.[14-16] The first BCPA simulations, which modeled this arrangement, showed that a forward flow of about two thirds of the systemic venous return (IVC flow) interferes minimally with the mean SVC pressure, with less pulsatility in the right pulmonary artery than the left.

There are multiple theoretic applications of CFD to cardiovascular surgery. Pressure gradients and aneurysmal formations after vascular patch enlargements are no doubt related to wall stresses resulting from the geometry and the material properties of the patches. This has been demonstrated in an elegant study with CFD technology on aortic wall stress profile after repair of coarctation of the aorta.[17] Computation of ventricular flow dynamics will open the field for numerous CFD studies in areas such as outflow tract patch enlargement, repair of ventricular aneurysms, repair and replacement of atrioventricular valves, and designs of

ventricular-assist devices. Preliminary comparative CFD studies of multiple sequential anastomoses versus simple end-to-side anastomosis in coronary revascularization have demonstrated the superiority of the former procedures (Menicanti L. Personal communication, 1995). Flow dynamic studies of stented arteries could help to predict restenosis and late outcomes, and could contribute to the design of new devices. There is little doubt that obstruction and attrition of extracardiac valved conduits are in great part related to local flow fields determined by the configuration of the anastomosis to the ventricular chamber and the distal vessel, the position of the valve, and the presence or absence of external compression. CFD and FEM can help in the understanding of the mechanics of vascular catastrophes such as atherosclerotic plaque rupture, a common cause of acute myocardial infarction, or shear failure as a cause of acute aortic dissection.[18, 19]

With regard to the future, one could foresee that with increasingly powerful computers FEM could be used to investigate mechanical stress at a cellular level. The body of knowledge describing the ability of cells to respond to mechanical stresses at a molecular level is growing rapidly.[18, 20] The endothelium functions as a mechanically sensitive signals-transduction interface between blood and vascular wall.[21] Changes in shear stress may lead to changes in cell shape, growth, and function, and in a wide variety of gene regulatory events. Are rheology and cellular and molecular biology going to meet in the near future? Such a convergence would open an area of fascinating research.

REFERENCES

1. de Leval MR, Kilner P, Gewillig M, Bull C. Total cavopulmonary connection: a logical alternative to atriopulmonary connection for complex Fontan operations. J THORAC CARDIOVASC SURG 1988;96:682-95.
2. Dubini G, de Leval MR, Pietrabissa R, Montevecchi FM, Fumero R. A numerical fluid mechanical study of repaired congenital heart defects: application to the total cavopulmonary connection. J Biomech [In press].
3. Migliavacca F, de Leval MR, Dubini G, Pietrabissa R, Montevecchi FM, Fumero R. Hemodynamics in the bidirectional cavopulmonary anastomosis: 3-D pulsatile numerical study. In: Proceedings of the 1995 bioengineering conference. Hochmuth RM, Langrana NA, Hefzy MS, eds. New York: The American Society of Mechanical Engineers, 1995: vol 29, 463-4.
4. Low HT, Chew YT, Lee CN. Flow studies on atriopulmonary and cavopulmonary connections of Fontan operations for congenital heart defects. J Biomed Eng 1993;15:303-7.
5. Nerem RM, Seed WA. An in vivo study of aortic flow disturbances. Cardiovasc Res 1972;6:1-14.
6. Avanzolini G, Barbini B, Cappello A, Cevenini G. CADCS simulations of the closed-loop cardiovascular system. Int J Biomed Comput 1987;22:33-49.
7. Janz R, Grimm A. Finite element method for the mechanical behaviour of the left ventricle. Circ Res 1972;30:244-52.
8. Idelsohn S, Costa L, Ponso R. A comparative computational study of blood flows through prosthetic heart valves using the finite element method. J Biomech 1985;18:97-115.
9. Pietrabissa R, Inzoli F, Fumero R. Simulation study of the fluid dynamics of aortocoronary bypass. J Biomed Eng 1990;12:419-24.
10. Rebergen S, Ottenkamp J, Doornbos J, Van der Well E, Chin J, de Ross A. Postoperative pulmonary flow dynamics after Fontan surgery: Assessment with nuclear magnetic resonance velocity mapping. J Am Coll Cardiol 1993;21:123-31.
11. Lins R, Lins M, Cavalcanti C, Miranda R, Mota J. Orthoterminal correction of congenital heart disease: double cavopulmonary anastomosis. J THORAC CARDIOVASC SURG 1982; 84:633-5.
12. Mainwaring RD, Lamberti JJ, Uzark K, Spicer RL. Bidirectional Glenn: is accessory pulmonary blood flow good or bad? [Abstract] Circulation 1994;90(Suppl 1):421.
13. Frommelt MA, Frommelt PC, Berger S, et al. Does an additional source of pulmonary blood flow alter outcome after a bidirectional cavopulmonary shunt? [Abstract] Circulation 1994;90(Suppl 1):422.
14. Billingsley A, Laks H, Boyce S, George B, Santuli T, Williams P. Definitive repair in patients with pulmonary atresia and intact ventricular septum. J THORAC CARDIOVASC SURG 1989;97:746-54.
15. Alvarado D, Sreeman N, McKay R, Boyd I. Cavopulmonary connection in repair of atrioventricular septal defect with small right ventricle. Ann Thorac Surg 1993;55:729-56.
16. Muster A, Zales W, Ilbawi M, Backer C, Duffy E, Mavroudis C. Biventricular repair of hypoplastic right ventricle assisted by pulsatile bidirectional cavopulmonary anastomosis. J THORAC CARDIOVASC SURG 1993;105:112-9.
17. McGiffin D, McGiffin P, Golbraith A, Cross R. Aortic wall stress profile after repair of coarctation of the aorta: is it related to subsequent true aneurysm formation? J THORAC CARDIOVASC SURG 1992;104:924-31.
18. Lee R, Kamm R. Vascular mechanics for the cardiologist. J Am Coll Cardiol 1994;23:1289-95.
19. Cheng G, Loree H, Kamm R, Fishbein M, Lee R. Distribution of circumferential stress in ruptured and stable atherosclerotic lesions. Circulation 1993;87:1179-87.
20. Wang N, Butler J, Ingber D. Mechano-transduction across the cell surface and through the cyto-skeleton. Science 1993;260:1124-7.
21. Davies P, Tripathi S. Mechanical stress mechanisms and the cell: an endothelial paradigm. Circ Res 1993;72:239-45.
22. Fung YC. Biodynamics: circulation. New York: Springer-Verlag, 1984.
23. Oddou C, Flaud P, Geiger D. Model of non-linear viscoelastic wall rheology applied to arterial dynamics. In: Bauer RD, Busse R, eds. The arterial system. Berlin: Springer, 1978:101-8.

Discussion

Dr. Aldo R. Castaneda *(Genolier, Switzerland).* We are once more indebted to Dr. de Leval and his bioengi-

neering colleagues for exposing us first to up-to-date technology in CFM and FEM and second to the application of these powerful investigative tools to the practice of cardiovascular surgery. I think that the simple but effective modification of adding a right-sided augmentation patch plasty to the cardiac segment of the SVC–right pulmonary artery anastomosis, an outgrowth of the effort of achieving the best possible balance between flow distribution and energy dissipation, exemplifies this effort. In addition, this modification should make the so-called unidirectional cardiopulmonary connection proposed by Laks unnecessary, retaining the hemodynamic advantages and much lower risk of formation of arteriovenous fistulas.

I was surprised that this methodology did not identify energy dissipation of IVC blood passing the SVC–right atrial junction. We know that the area ratio between the IVC–right atrial junction and SVC–right atrial junction is about 2:1 because the orifice size or area size of the IVC–right atrial junction is about twice as large as that of the SVC.

It appears to me that the augmentation plasty goes through the SVC–right atrial junction. Could you comment on that? Clearly the concept of allowing pulsatile forward pulmonary flow, either through a stenotic pulmonary valve or through a systemic artery–pulmonary artery shunt, is an option, particularly for patients who are not ideal candidates for a Fontan operation.

I am sure that we will hear much more from your group after you have been able to unravel the remaining problems of various pulmonary vascular geometries and also bilateral pulmonary parenchymal flow distribution.

Dr. de Leval. It is true that the patch goes down, across the narrowest part of the pathway, but the more I look at flow simulations the more I believe that maintaining streamlining is more important than the actual diameter. I think a smooth, progressive reduction of diameter of a pathway is less important or deleterious than the loss of streamlining.

Dr. Serafin Y. DeLeon *(Maywood, Ill.).* I was just wondering whether you have already done some preliminary studies in patients in terms of the total cavopulmonary anastomosis in which you have straddled a little bit to the right pulmonary artery, whether you have correlated this with lung scan studies and demonstrated that the flow really goes where you intend it to go and determined the clinical implications of your model.

Dr. de Leval. It is an important question. Obviously, all these results have to be validated, and we are in the process of validating them by using magnetic resonance imaging to look at flow distribution to the two lungs.

Dr. Richard A. Jonas *(Boston, Mass.).* Do you have any thoughts on differences in hemodynamics that might result from the use of different materials? For example, there seems to be a lot of enthusiasm right now for prosthetic extracardiac conduits. There also has been a suggestion of using a pedicled pericardial graft that is placed along the external surface of the right atrium, with the implication being that pulsatility is induced by this. Have you looked at any of these other alternatives?

Dr. de Leval. We have not compared the flow dynamics through different materials used to construct the IVC pathway. I am aware of the recent enthusiasm for extracardiac conduits to channel the IVC blood to the pulmonary artery but cannot comment on the advantages of, for example, a pericardial graft sewn on the outside of the heart.

Appendixes

Appendix 1. The basic equations of fluid mechanics consist of the equation of continuity, which expresses the law of conservation of mass, the equation of motion, which expresses the law of conservation of momentum, the equation of balance of energy, and the constitutive equation and boundary conditions. If there is no heat input into the system and no heat source in the region, the equation for balance of energy is the same as that for balance of mechanical energy and work; it leads to no new independent equation. Let us consider an incompressible Newtonian viscous fluid. Let x, y, and z be rectangular Cartesian coordinates. Let the velocity components along the x-, y-, and z-axis directions be denoted by u, v, and w, respectively. Let p denote pressure. Let μ and ρ denote the coefficient of viscosity (constant for a Newtonian fluid) and the density of the fluid (constant for an incompressible fluid), respectively.

The condition of incompressibility reduces the equation of continuity to the following equation:

$$\frac{\partial u}{\partial x} + \frac{\partial v}{\partial y} + \frac{\partial w}{\partial z} = 0 \qquad \text{(A1.1)}$$

The equation of motion is a vectorial equation. For an incompressible Newtonian viscous fluid, the (scalar) correspondents in the x-, y-, z-axis directions are named *Navier-Stokes* equations. They are written as follows:

$$\rho\left(\frac{\partial u}{\partial t} + u\frac{\partial u}{\partial x} + v\frac{\partial u}{\partial y} + w\frac{\partial u}{\partial z}\right) = X - \frac{\partial p}{\partial x} + \mu\left(\frac{\partial^2 u}{\partial x^2} + \frac{\partial^2 u}{\partial y^2} + \frac{\partial^2 u}{\partial z^2}\right) \qquad \text{(A1.2)}$$

$$\rho\left(\frac{\partial v}{\partial t} + u\frac{\partial v}{\partial x} + v\frac{\partial v}{\partial y} + w\frac{\partial v}{\partial z}\right) = Y - \frac{\partial p}{\partial y} + \mu\left(\frac{\partial^2 v}{\partial x^2} + \frac{\partial^2 v}{\partial y^2} + \frac{\partial^2 v}{\partial z^2}\right) \qquad \text{(A1.3)}$$

$$\rho\left(\frac{\partial w}{\partial t} + u\frac{\partial w}{\partial x} + v\frac{\partial w}{\partial y} + w\frac{\partial w}{\partial z}\right) = Z - \frac{\partial p}{\partial z} + \mu\left(\frac{\partial^2 w}{\partial x^2} + \frac{\partial^2 w}{\partial y^2} + \frac{\partial^2 w}{\partial z^2}\right) \qquad \text{(A1.4)}$$

In equations A1.2 to A1.4, each term has a physical meaning. Let us consider equation A1.2 *(x*-axis direction) and examine its terms: $\rho\left(\partial u / \partial t\right)$ represents the "transient" inertia force per unit volume of fluid; that is, the result of the change of u velocity component in the generic point $P(x,y,z)$ in time. $\rho\left(u\partial u / \partial x + v\partial u / \partial y + w\partial u / \partial z\right)$ represents the "convective" inertia force per unit volume of fluid; that is, the result of the change of u

velocity component in the neighborhood of the generic point P(*x,y,z*) in the *x*-, *y*-, *z*-axis directions. $\partial p/\partial x$ represents the force per unit volume caused by the presence of a pressure gradient in the *x*-axis direction. $\mu(\partial^2 u/\partial x^2 + \partial^2 u/\partial y^2 + \partial^2 u/\partial z^2)$ represents the force per unit volume due to the viscous friction. *X* represents the component of the body forces (e.g., gravity force) per unit volume of fluid in the *x*-axis directions.

Equations A1.1 to A1.4 can be solved only if appropriate boundary conditions are specified. Boundary conditions are typically expressed as velocity or pressure distributions on some portion of the boundary that delimits the fluid domain. To characterize an incompressible viscous flow, two dimensionless parameters are often used. They are the Reynolds number (Re) and the Womersley number (Wo). They are defined as follows:

$$\mathrm{Re} = \frac{\text{convective inertia force}}{\text{viscous friction force}} = \frac{\rho V D}{\mu} \qquad \text{(A1.5)}$$

$$\mathrm{Wo} = \frac{\text{transient inertia force}}{\text{viscous friction force}} = \frac{D}{2}\sqrt{\frac{2\pi\rho f}{\mu}} \qquad \text{(A1.6)}$$

where ρ and μ are density and viscosity of the fluid and *D, V, f* are the diameter of the vessel, the mean velocity of the flow, and the frequency of pulsation, respectively. In a steady flow, the transient inertial force vanishes; the first term in equations A1.2 to A1.4 is therefore dropped and Wo is 0.

At low Re, a steady flow is laminar and transition from laminar to turbulent flow occurs when the critical Re is reached. In a pulsatile flow, this threshold also depends on the rate of change of velocity and therefore on the Wo. For full details, the reader is urged to see basic fluid dynamics textbooks (for instance Fung[22]).

Appendix 2

Three-dimensional FEM models. This article reports results from two distinct classes of computer simulations:

- Steady-state simulations in the TCPC studies.
- Pulsatile simulations in the BCPA studies (because of the pulsatile forward flow in the main pulmonary artery).

Vessel diameters in TCPC models are as follows: SVC diameter (D_{SVC}), 1.2 cm; IVC diameter (D_{IVC}), 1.5 cm; left pulmonary artery diameter (D_{LPA}), 1.0 cm; and right pulmonary artery diameter (D_{RPA}), 1.0 cm. In BCPA models, diameters are as follows: D_{SVC}, 1.5 cm; pulmonary artery diameter (D_{PA}) 1.5 cm; D_{LPA}, 1.2 cm; and D_{RPA}, 1.2 cm.

General assumptions adopted for the CFD study described here are as follows: (1) terms *X, Y, Z* (body forces per unit volume) discarded in Navier-Stokes equations, (2) incompressible homogeneous Newtonian fluid ($\rho = 1.06 \times 10^3$ kg/m^3, $\mu = 3 \times 10^{-3}$ kg · m^{-1} · sec^{-1}), (3) rigid and impermeable vessel walls, (4) all vessel axes assumed to lie in the same plane (geometric symmetry plane).

Assumption 3 is quite unusual in hemodynamic studies related to arterial districts because flow pulsatility cannot usually be discarded. It is a fairly correct hypothesis in this study of the TCPC, however, because the right atrium and ventricle are totally bypassed and both the incoming flows are from venous districts. Changes in caval flows and pressures caused by both respiratory rhythm and geometry-dependent fluid dynamic effects are discarded as well. As a consequence, the vessel diameters can be assumed to remain constant and the hypothesis of rigid walls is reasonable. Such an assumption appears less reasonable for the study of the BCPA. In fact, nonlinear and viscoelastic properties of pulmonary arterial walls have effects on the details of local flow pattern, but shear stresses, for example, are not significantly altered.[23] If the pressure gradient is low, as encountered in these vessels, the local fluid dynamics will be slightly influenced, and the results obtained with a rigid model are expected not to differ greatly from the real ones.

Assumption 4 allowed us to represent only half of the model, with an important reduction in the storage and memory requirements for computations. The geometry of the developed three-dimensional models is clearly the result of a compromise between the requirement of describing accurately the highly complex anatomy of the pulmonary bifurcation and caval anastomoses and the necessity of using a modular geometric structure that can be automatically created or adapted through a custom-written FORTRAN computer program. We believe that this limitation does not affect the evaluation of the different hemodynamic designs from a comparative point of view. Regarding the boundary conditions for the models, they were adopted as follows:

- No-slip condition at the walls (velocity equal to zero).
- Fully developed velocity profiles at the inlet sections (SVC and IVC) in the TCPC studies:

$$V_i = V_{max,i}\left(1 - \frac{4}{D_i^2}x^2 - \frac{4}{D_i^2}y^2\right) \quad (i = \mathrm{IVC, SVC}) \qquad \text{(A2.1)}$$

being $V_{max,i}$, *x* and *y* the peak velocity and the two current coordinates in a Cartesian system for each inlet section, respectively, assumed circular.

- Flat velocity profile at the inlet section of the main pulmonary artery in the BCPA studies. The volume flow rate changes as a sinusoidal curve during systole and is zero during diastole. SVC inlet flow is the same as in TCPC studies.
- Symmetry boundary condition applied at the symmetry plane; that is, in every point of the symmetry plane the normal velocity component V_n is constrained to be zero while the two tangent components are left free.
- Uniform pressure at the outlet sections (left and right pulmonary arteries): the actual value is computed coupling the three-dimensional model with the lumped-parameter model of the pulmonary circulation by means of an iterative procedure.

Lumped-parameter model. The lumped-parameter model is a mechanical model of the pulmonary circulation that represents the two lungs and the left atrium in terms of lumped components. To simplify computations, only resistance components appear in this model; both elastic compliances and inertial effects are absent. Left atrial pressure

(P_{LA}) is assumed to be constant and to equal the mean pressure measured during cardiac catheterization. The left atrium is thus assumed to behave like a constant-pressure reservoir. Cardiac catheterizations have also supplied the value of global pulmonary resistance for the model, equally split into two parallel resistances *(R_{Lung})* corresponding to the two lungs, assuming that both lungs offer the same resistance. Inputs for this model are the volumetric flow rates $Q_{LPA} = Q_{LUPA} + Q_{LLPA}$ and $Q_{RPA} = Q_{RUPA} + Q_{RLPA}$ (where *Q* is flow and *LPA* is left pulmonary artery, *LUPA* is left upper pulmonary artery, *LLPA* is left lower pulmonary artery, *RPA* is right pulmonary artery, *RUPA* is right upper pulmonary artery, and *RLPA* is right lower pulmonary artery) computed with the three-dimensional model. It yields the pressure values P_{LPA} and P_{RPA} in the two pulmonary branches corresponding to the assigned flow rates:

$$P_i = P_{LA} + R_{Lung}Q_i \quad (i = LPA, RPA) \qquad (A2.2)$$

These values are then used as new boundary conditions of the FEM three-dimensional model in the next FIDAP run.

Energy-loss indexes (for TCPC simulations only). For a quantitative evaluation of the results in terms of the best hemodynamic design for the TCPC, two energetic indexes (related to the whole three-dimensional fluid dynamic domain) have been adopted. These are the hydraulic dissipated power *($\dot{W}_{diss}$)* and the total energy-loss coefficient *(C_e,* dimensionless coefficient). Total energy includes both kinetic and pressure energy. Their meanings are as follows:

$$\dot{W}_{diss} = \dot{W}_{in} - \dot{W}_{out}$$

where $\dot{W}_{in}$ is rate at which total energy is carried by the fluid entering the model and $\dot{W}_{out}$ is rate at which total energy is carried by the fluid leaving the model.

$$C_e = \frac{\dot{W}_{diss}}{\text{rate of kinetic energy carried by fluid entering model}}$$

and their mathematic expressions are as follows:

$$\dot{W}_{diss} = \left(\frac{1}{2}\rho V_{IVC}^2 + P_{IVC}\right)Q_{IVC} + \left(\frac{1}{2}\rho V_{SVC}^2 + P_{SVC}\right)Q_{SVC} - \sum_i \left(\frac{1}{2}\rho V_i^2 + P_i\right)Q_i \qquad (A2.3)$$

$$C_e = \frac{\left(\frac{1}{2}\rho V_{IVC}^2 + P_{IVC}\right)Q_{IVC} + \left(\frac{1}{2}\rho V_{SVC}^2 + P_{SVC}\right)Q_{SVC} - \sum_i \left(\frac{1}{2}\rho V_i^2 + P_i\right)Q_i}{\frac{1}{2}\rho(V_{IVC}^2 Q_{IVC} + V_{SVC}^2 Q_{SVC})} \qquad (A2.4)$$

where P_i and V_i *(i* is *LUPA, RUPA, LLPA, RLPA)* represent the mean pressure and velocity respectively on each outlet section and P_{IVC}, P_{SVC}, Q_{IVC}, and Q_{SVC} represent the mean pressure and velocity, respectively, on each inlet section.

In the definition of the loss coefficient C_e, the kinetic energy rate entering the three-dimensional model (inlet sections of the two venae cavae) has been used to obtain a dimensionless coefficient. It is important to note that this amount of energy rate remains constant in all the TCPC simulations because both vessel diameters and inlet flow rates are left unchanged. This allows quantitative comparison of the different geometric designs for the TCPC.